Generic Contrast Agents
Our portfolio is growing to serve you better. Now you have a *choice*.
FRESENIUS KABI
VIEW CATALOG

AJNR

Nodular Fasciitis in the Head and Neck: CT and MR Imaging Findings

Sung Tae Kim, Hyung-Jin Kim, Sun-Won Park, Jung Hwan Baek, Hong Sik Byun and Young Mo Kim

AJNR Am J Neuroradiol 2005, 26 (10) 2617-2623
http://www.ajnr.org/content/26/10/2617

This information is current as of May 25, 2025.

AJNR Am J Neuroradiol 26:2617–2623, November/December 2005

Nodular Fasciitis in the Head and Neck: CT and MR Imaging Findings

Sung Tae Kim, Hyung-Jin Kim, Sun-Won Park, Jung Hwan Baek, Hong Sik Byun, and Young Mo Kim

BACKGROUND AND PURPOSE: **The purpose of this study was to describe the CT and MR imaging findings of nodular fasciitis occurring in the head and neck region.**

METHODS: **CT ($n = 6$) and MR ($n = 4$) images obtained from 7 patients (3 men and 4 women; mean age, 19.4 years; age range, 1–48 years) with surgically confirmed nodular fasciitis in the head and neck were retrospectively reviewed. All patients presented with a palpable mass in the head and neck that was noticed 1–3 months earlier: 5 in the face, one in the occipital scalp, and the remaining one in the supraclavicular fossa. We investigated the CT and MR imaging characteristics with emphasis on the location, size, internal content, margin, enhancement pattern, and signal intensity of the lesion.**

RESULTS: **All lesions appeared as a discrete mass on imaging, ranging from 1.0 cm to 4.6 cm in diameter (mean, 2.2 cm). Six lesions, all of which appeared benign, were located in the subcutaneous tissue superficial to the deep cervical fascia. The remaining lesion was located deep to the temporalis muscle and showed an aggressive imaging appearance, markedly eroding the bony orbit and skull. Five lesions were solid, and 2 lesions were partly or completely cystic in appearance. Five lesions were well defined, whereas 2 lesions were ill defined. Four of 5 solid lesions showed moderate to marked diffuse enhancement, whereas the remaining lesion demonstrated mild enhancement. Two cystic lesions showed peripheral, nodular, or rimlike enhancement. Compared with muscle, both solid lesions had isointense signal intensity on T1-weighted images and hyperintense signal intensity on T2-weighted images, whereas the signal intensity of the solid portions of the deep-seated, partly cystic lesion was isointense on both T1-weighted and T2-weighted images.**

CONCLUSION: **Although rare, nodular fasciitis occurs as a discrete solid or cystic mass in the head and neck, depending on the predominant stromal components. When one sees a head and neck mass with a superficial location and moderate to marked enhancement on CT and MR imaging, nodular fasciitis should be included in the differential diagnosis, especially in patients with a recently developed, rapidly growing mass and a history of recent trauma.**

Nodular fasciitis is a benign proliferative lesion of fibroblasts with pseudosarcomatous histologic features. It usually arises in the subcutaneous tissues with the most common location being the upper extremities, followed by the head and neck, the lower extremities, and trunk in decreasing order (1, 2). Both clinically and histologically, it is not infrequent to misdiagnose nodular fasciitis as a malignant tumor, especially as a sarcomatous lesion, because it frequently grows very rapidly without evidence of associated infection and shows histologic findings similar to those seen in malignant tumors, such as high cellularity, increased mitotic activity, and infiltrative growth pattern. Although the radiologic features of nodular fasciitis are well described (1, 3–5), discussion of nodular fasciitis in the head and neck is relatively sparse. The purpose of this study was to describe the CT and MR imaging findings of nodular fasciitis occurring in the head and neck region.

Received March 7, 2005; accepted after revision May 9.

From the Departments of Radiology (S.T.K., H.J.K., H.S.B.) and Otolaryngology and Head and Neck Surgery (J.H.B.), Samsung Medical Center, Sungkyunkwan University School of Medicine, Seoul, Korea; and the Departments of Radiology (S.T.K., H.J.K., S.W.P.) and Otorhinolaryngology (Y.M.K.), Inha University College of Medicine, Incheon, Korea.

Address correspondence to H.J. Kim, Department of Radiology, Samsung Medical Center, Sungkyunkwan University School of Medicine, 50 Ilwon-Dong, Kangnam-Ku, Seoul 135-710, Korea.

© American Society of Neuroradiology

Methods

Patients

The review of medical records revealed 7 patients with surgically confirmed nodular fasciitis in the head and neck who

Clinical and imaging findings in 7 patients with nodular fasciitis in the head and neck

Patient No./ Age/Sex	Chief Complaint	Physical Examination	Trauma History	CT Scan	MR Image	Location	Size* (cm)	Shape	Content	Signal Intensity on MR Imaging		Enhancement Pattern
										T1WI	T2WI	
1/48 y/F	Recurrent preauricular mass for 3 mo	Rubbery hard, nontender, movable	Yes	Yes	No	Periparotid subcutaneous tissue	1.0	Round, ill defined	Solid	—	—	Mild heterogeneous enhancement
2/18 y/F	Rapidly growing cheek mass for 3 mo	Rubbery hard, nontender, movable	No	Yes	No	Lateral malar area beneath zygomaticus major muscle	1.8	Ovoid, well defined	Solid	—	—	Marked heterogeneous enhancement
3/14 mo/M	Perinasal mass for 1 mo with no significant growth	Rubbery hard, nontender, movable	No	Yes	Yes	Perinasal area beneath levator labii superioris muscle	2.0	Round, well defined	Completely cystic	Cystic portion slightly hyperintense	Hyperintense	Peripheral rim enhancement
4/35 y/M	Cheek mass for 1 mo with no significant growth	Rubbery hard, nontender, movable	No	No	Yes	Lateral malar area beneath zygomaticus major muscle	1.5	Ovoid, well defined	Solid	Isointense	Hyperintense	Moderate homogeneous enhancement
5/11 y/F	Rapidly growing supraclavicular mass for 3 mo	Rubbery hard, nontender, movable	No	Yes	Yes	Subcutaneous tissue of supraclavicular fossa	3.5	Ovoid, well defined	Solid	Isointense	Hyperintense	Marked homogeneous enhancement
6/22 y/F	Rapidly growing scalp mass for 1 mo	Rubbery hard, tender, movable	No	Yes	No	Subcutaneous tissue of occipital scalp	1.3	Oblong, well defined	Solid	—	—	Marked homogeneous enhancement
7/16 mo/M	Rapidly growing periorbital mass for 2 mo	Rubbery hard, nontender, fixed	Yes	Yes	Yes	Periorbital area deep to temporalis muscle	4.6	Ovoid, ill defined	Partly cystic	Solid portion isointense, cystic portion slightly hyperintense	Isointense	Peripheral nodular enhancement

* Size in greatest diameter.

formed the basis of this study. We retrospectively reviewed CT ($n = 6$) and MR ($n = 4$) images obtained from these 7 patients, one of whom was previously reported in the literature (6). There were 3 men and 4 women, ranging in age from 14 months to 48 years, with a mean age of 19.4 years. Three patients underwent both CT and MR examinations.

All patients presented with a palpable, tender ($n = 1$) or nontender ($n = 6$), rubbery hard, movable ($n = 6$) or fixed ($n = 1$) mass in the head and neck, which had first been noticed 1–3 months earlier, with an average duration of 2 months, and enlarged thereafter. Five patients had a mass in the face, including the lateral malar area in 2 patients and periparotid, perinasal, and periorbital areas in a single patient each. One patient had a mass on the occipital scalp, and a large mass was palpated at the supraclavicular fossa in the remaining one patient. The patient with a periorbital mass complained of progressive exophthalmos. Two patients had had a history of trauma before the lesions were developed—one with a periparotid mass and a history of face lifting 1 month earlier and the other with a periorbital mass and a history of falling down. There was no history of significant previous trauma obtainable in the remaining 5 patients.

Imaging Techniques

All CT examinations (6 patients) were performed on a spiral scanner (HiSpeed Advantage; GE Medical Systems, Milwaukee, WI) to produce postcontrast axial images with 3-mm collimation. In 4 patients, precontrast images were also obtained.

All MR examinations (4 patients) were performed on a 1.5T scanner (Signa Advantage Horizon; GE Medical Systems) to produce pre- and postcontrast T1-weighted spin-echo images and T2-weighted fast spin-echo images with or without fat saturation. Images were obtained in at least 2 planes with 3–4-mm section thickness and 0–1-mm intersection gap.

Image Analysis

We investigated the CT and MR imaging characteristics, with emphasis on the location, size, internal content, and margin of the lesion. The location of the lesion was categorized as subcutaneous, intramuscular, and fascial according to the anatomic location in relation to the cervical fascia. The size of the lesion was measured at the greatest diameter of the lesion. As for the internal content, the lesion was divided into solid and cystic, where the "cystic" lesions were defined as those containing typical fluid-like attenuation or signal intensity on CT or MR imaging and also showed a nodular or rimlike enhancement on contrast-enhanced CT and MR imaging. The margin of the lesion was classified as well defined and ill defined. When the lesion had a focally serrated border (ie, notched in appearance, without evident perilesional infiltration), it was also classified as well defined. Density on precontrast CT scans and signal intensity on T1- and T2-weighted MR images were also documented, as were enhancement patterns on contrast-enhanced CT and MR imaging. The degree of enhancement was subjectively assessed as being mild, moderate, and marked. Imaging interpretation was conducted by a dedicated head and neck radiologist and a general neuroradiologist in conference, both of whom have been practicing for >10 years.

Results

The clinical and radiologic findings of 7 cases of nodular fasciitis are summarized in the Table. All lesions appeared as a discrete mass on imaging. Six lesions were located in the subcutaneous tissue superficial to the deep cervical fascia (subcutaneous type; Figs 1–3). Of them, 3 lesions were located just beneath the muscles of facial expression. These subcutaneous lesions were benign in appearance. One lesion was located deep to the temporalis muscle (intramuscular type). This lesion was the largest one included in this study and showed an aggressive imaging appearance, causing marked erosion of the bony orbit and skull (Fig 4). The lesion size ranged from 1.0 cm to 4.6 cm in greatest diameter with a mean of 2.2 cm. Five lesions were solid (Figs 1 and 3), and 2 lesions—including one case of intramuscular type—were partly or completely cystic (Figs 2 and 4) in appearance. The margin of the lesion was well defined in 5 (Figs 1–3) and ill defined in 2 (Fig 4). Four of 5 solid lesions showed moderate to marked diffuse, homogeneous ($n = 3$; Fig 3) or heterogeneous ($n = 1$; Fig 1) enhancement, whereas the remaining lesion demonstrated mild heterogeneous enhancement. Two cystic lesions revealed peripheral, nodular, or rimlike enhancement (Figs 2 and 4). The adjacent cervical fascia was also enhanced in 4 lesions.

FIG 1. Case 2. Nodular fasciitis on the left lateral malar area in an 18-year-old man. Contrast-enhanced axial CT scan shows a well-defined ovoid soft tissue mass in the subcutaneous fat just beneath the zygomaticus major muscle (*arrow*). Note marked, though heterogeneous, enhancement of the lesion.

Compared with the adjacent muscle, the attenuation of the lesion seen on precontrast CT scans obtained in 4 patients was hypoattenuated in 2 patients and isoattenuated in 2 patients. No lesion contained calcification demonstrable on CT scans. Compared with muscle, both solid lesions showed isointense signal intensity on T1-weighted images and hyperintense signal intensity on T2-weighted images (Fig 3). The signal intensity of the solid portion of the deep-seated, partly cystic lesion was isointense to that of muscle on both T1- and T2-weighted images, whereas its cystic portion was slightly hyperintense and isointense to that of CSF on T1- and T2-weighted images, respectively (Fig 4). Compared with CSF, the cystic portion of the completely cystic lesion demonstrated slightly hyperintense signal intensity on T1-weighted images and isointense signal intensity on T2-weighted images (Fig 2).

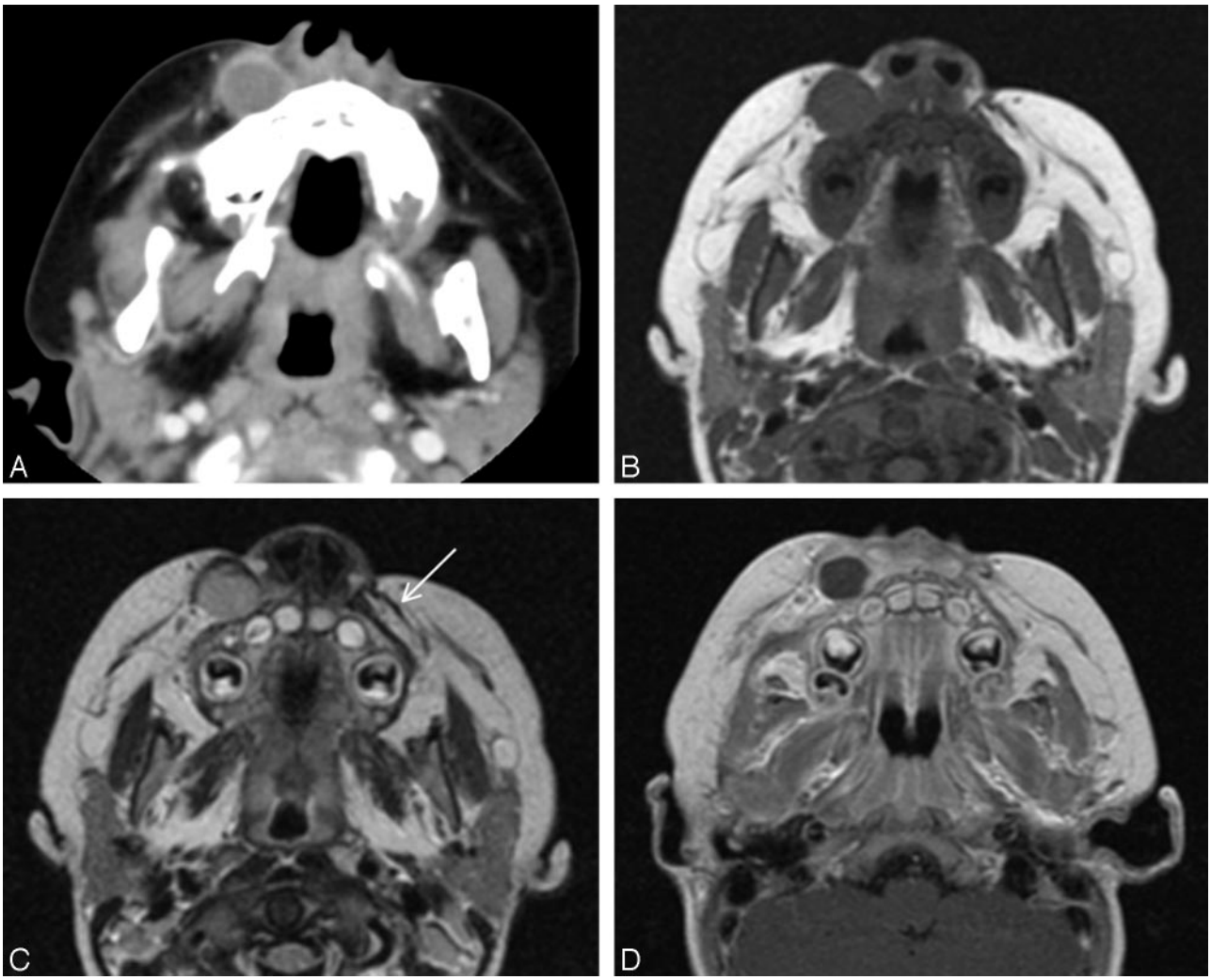

FIG 2. Case 3. Nodular fasciitis involving the right perinasal area in a 14-month-old boy.

Contrast-enhanced axial CT scan (*A*) and axial T1-weighted (*B*), T2-weighted (*C*), and contrast-enhanced T1-weighted (*D*) MR images show a well-defined, relatively thick-walled, round cystic mass in the subcutaneous fat just beneath the levator labii superioris muscle. *Arrow* in *C* indicates the same muscle in the contralateral cheek. Compared with CSF, the cystic portion of the lesion demonstrated slightly hyperintense signal intensity on T1-weighted image (*B*) and isointense signal intensity on T2-weighted image (*C*). Note peripheral rimlike enhancement of the lesion. The absence of imaging findings of associated infection, such as perilesional infiltration, edema, or enhancement does not favor the diagnosis of abscess.

Discussion

Nodular fasciitis is a benign tumor-like fibroblastic proliferation, also known as subcutaneous pseudosarcomatous fibromatosis, infiltrative fasciitis, or proliferative fasciitis. Other benign lesions of fibroblastic origin include congenital generalized fibromatosis, fibrous hamartoma of infancy, palmar and plantar fibromatosis, and musculoaponeurotic fibromatosis (7). The intermediate, well-differentiated, low-grade nonmetastasizing fibrosarcoma, also known as aggressive fibromatosis, and the most aggressive poorly differentiated fibrosarcoma represent the malignant end of the spectrum of fibrous lesions (7–9). Although several mechanisms were proposed including reactive or inflammatory process, the pathogenesis of nodular fasciitis is still unknown (7–9). Antecedent trauma has been suggested as an inciting factor. Only a minority of cases, however, have been reported to be associated with trauma (1, 3, 10). In this study, 2 of 7 cases were associated with trauma.

Nodular fasciitis can be found anywhere in the body and is equally common in men and women. The most common site of involvement is the upper extremity (48%), especially the volar aspect of the forearm, followed by trunk (20%), head and neck (15%–20%), and lower extremities (15%) (3, 7, 11). Although any age group can be affected, young adults between 20 and 40 years are most commonly involved. Fewer than 20% of cases occur at the age <20 years and only 5% in patients >70 years of age (1, 2, 7, 10, 12). In contrast, our study population was significantly younger than those previously reported. The mean age of our study population was 19.4 years with >50% (4/7) <20 years of age. Furthermore, 2 patients were only 1 year of age. The selection bias due to the small number of cases probably caused these demographic discrepancies between the studies.

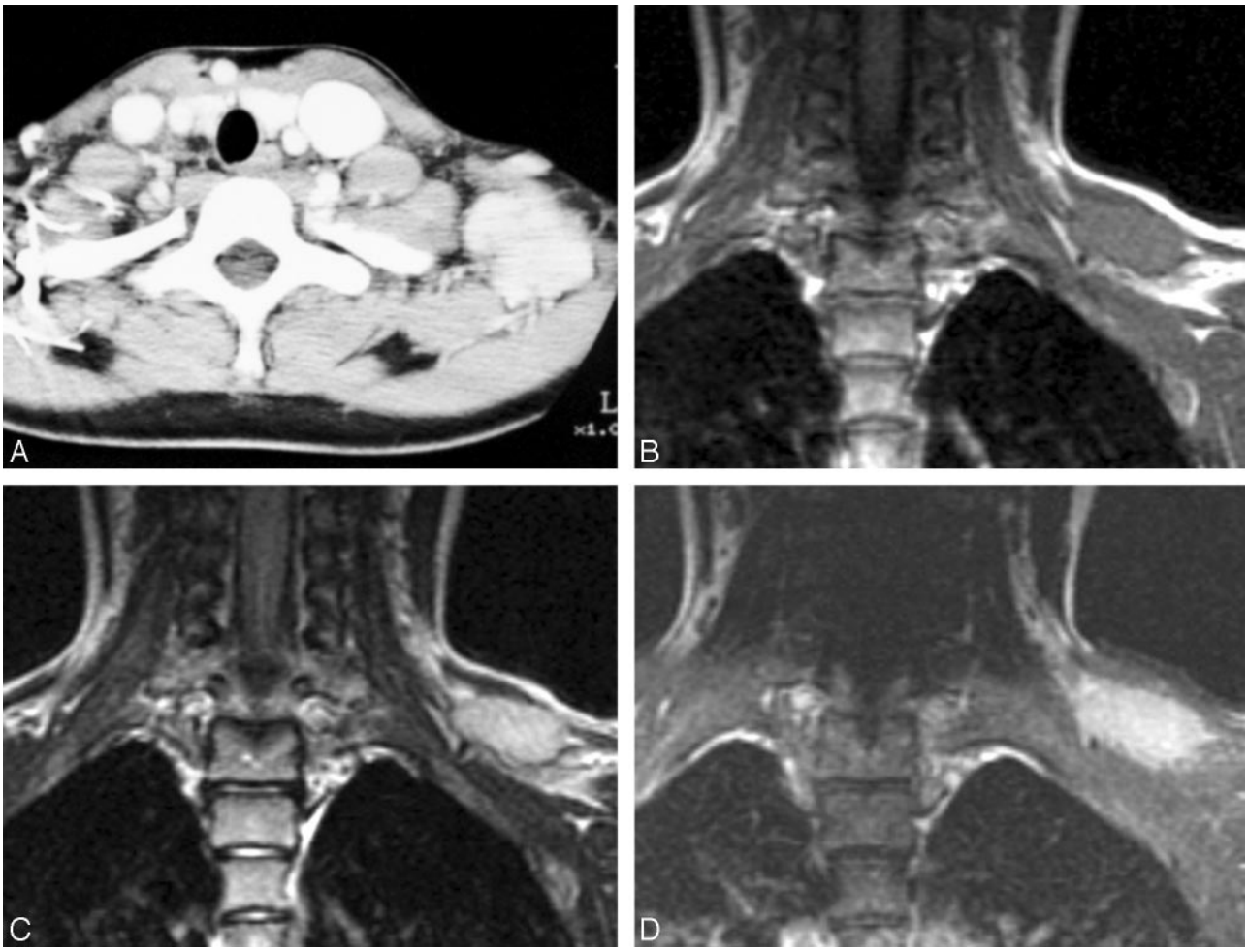

FIG 3. Case 5. Nodular fasciitis in the left supraclavicular fossa in an 11-year-old girl.

Contrast-enhanced axial CT scan (*A*) and coronal T1-weighted (*B*), T2-weighted (*C*), and contrast-enhanced fat-suppressed T1-weighted (*D*) MR images show a markedly enhancing, well-defined, ovoid soft tissue mass in the subcutaneous fat of the left supraclavicular fossa. The lesion has a partly serrated border on contrast-enhanced MR image (*D*). Compared with the adjacent muscle, the mass is isointense and significantly hyperintense on T1- (*B*) and T2-weighted (*C*) images, respectively.

The most common clinical presentation of nodular fasciitis is a solitary, rapidly growing mass with frequently associated pain and tenderness. Less frequently, compression of peripheral nerve can cause numbness, paresthesia, and shooting pain (3, 4). Multiple lesions are extremely rare. The size of the lesions can vary from 0.5 cm to 10 cm, but most are <4 cm (1, 3, 4, 12). Larger lesions are exceptional. There are 3 subtypes of nodular fasciitis according to the anatomic location: subcutaneous, intramuscular, and intermuscular (fascial) types. The subcutaneous type occurs 3–10 times more commonly than the other subtypes and presents as a subcutaneous nodule. The intramuscular type is most likely to mimic a soft tissue malignancy because it is typically larger in size and deeper in location. The intermuscular type is less well circumscribed and grows along the fascial planes (1, 3–5, 11, 12). Rare subtypes include intravascular and intradermal forms (3). The clinical manifestations of our study population were generally similar to those of the previous reports. Six of 7 cases, all of which were <4 cm in diameter, fell into the subcutaneous type. The remaining case with its diameter >4 cm was categorized as the intramuscular type. Concerning the growth rate of nodular fasciitis, though some reports documented the propensity of slow or no growth during follow-up (1), most the reported cases were prone to rapid growth, as seen in 4 of 7 cases in this study.

Macroscopically, nodular fasciitis is a nonencapsulated, tan to gray-white, round or oval mass. Microscopically, it is characterized by plump, immature-appearing fibroblasts and a variable amount of mature birefringent collagen. The fibroblasts are arranged in short irregular bundles and fascicles and are accompanied by an attenuated reticulin meshwork. Mitotic figures without atypical mitoses are common (8). The intervening matrix tends to be abundant, loose, and myxoid. Recognizable vascularity often is present, and areas resembling reparative tissue and inflammation are common (1, 13).

Nodular fasciitis can also be classified into myxoid, cellular, and fibrous subtypes on the basis of the amount and type of extracellular matrix. A relationship has been proposed between these subtypes and the age of the lesion: the younger the lesion, the more

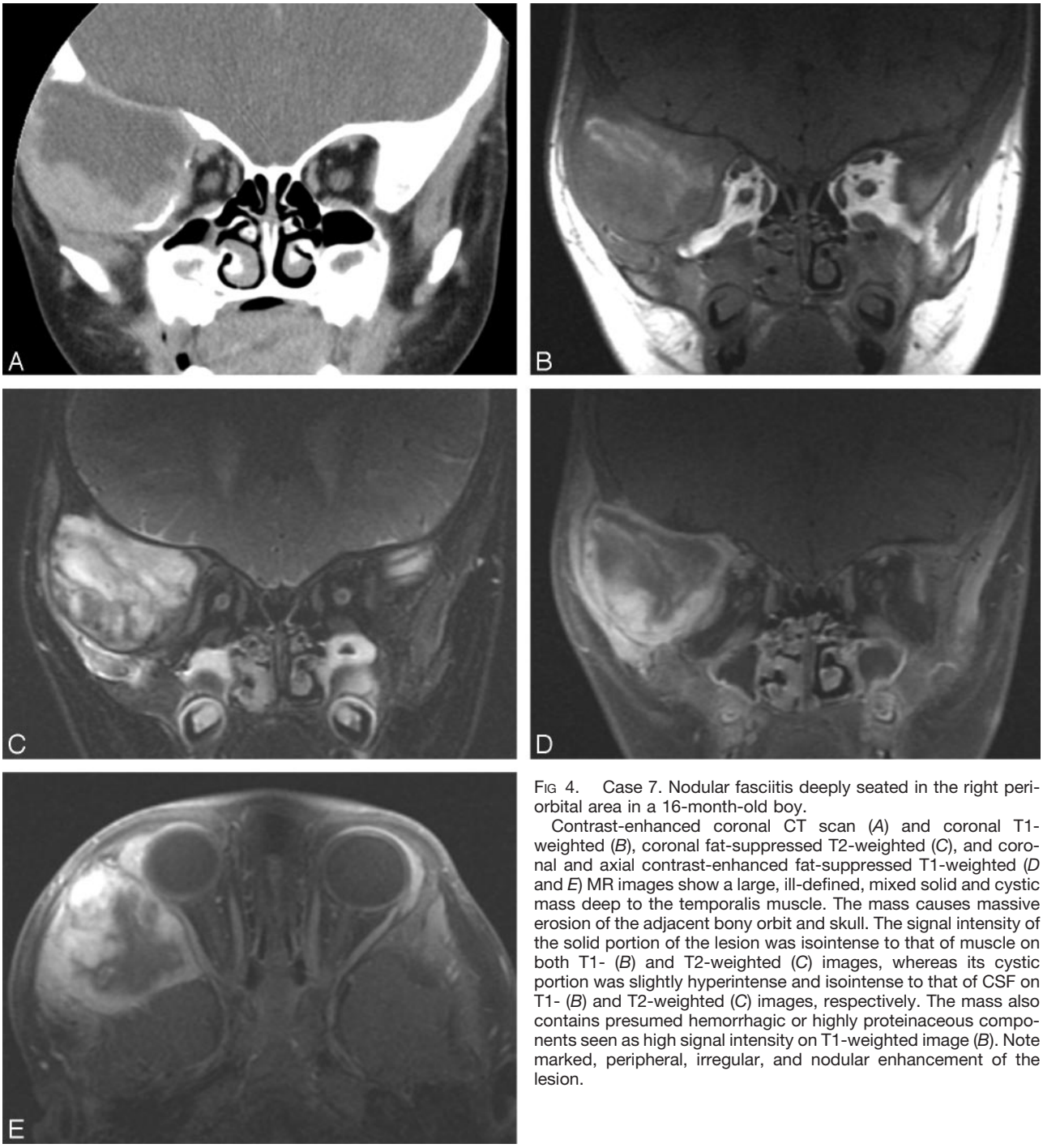

FIG 4. Case 7. Nodular fasciitis deeply seated in the right periorbital area in a 16-month-old boy.

Contrast-enhanced coronal CT scan (*A*) and coronal T1-weighted (*B*), coronal fat-suppressed T2-weighted (*C*), and coronal and axial contrast-enhanced fat-suppressed T1-weighted (*D* and *E*) MR images show a large, ill-defined, mixed solid and cystic mass deep to the temporalis muscle. The mass causes massive erosion of the adjacent bony orbit and skull. The signal intensity of the solid portion of the lesion was isointense to that of muscle on both T1- (*B*) and T2-weighted (*C*) images, whereas its cystic portion was slightly hyperintense and isointense to that of CSF on T1- (*B*) and T2-weighted (*C*) images, respectively. The mass also contains presumed hemorrhagic or highly proteinaceous components seen as high signal intensity on T1-weighted image (*B*). Note marked, peripheral, irregular, and nodular enhancement of the lesion.

myxoid component it contains. In contrast, if the lesion is mature, more fibrotic component is likely to be contained (3, 12). Although differentiation from other fibrous tumors, such as fibromatosis, fibrous histiocytoma, and fibrosarcoma, is not always easy, nodular fasciitis tends to be more circumscribed with a higher mitotic activity, a greater resemblance to granulation tissue, and an increased myxoid matrix (1).

On CT and MR imaging, nodular fasciitis is generally seen as a relatively well-defined, soft-tissue mass of superficial location (1, 14, 15). Deep-seated lesions, mostly of intramuscular type, tend to be large and have ill-defined margins (1). Although histologically benign, the deep-seated lesions may show an aggressive clinical behavior simulating a malignancy. These can invade and destroy the adjacent structures including the bone, as seen in cranial fasciitis which is a rare variant of nodular fasciitis and causes destruction of the outer tables of the skull in most cases (14). In the present study, 5 of 7 cases were well defined, and the remaining 2 lesions were ill defined. One case of intramuscular type was embedded deep in the temporalis muscle and caused marked erosion of the

bony orbit and skull. Although various degrees of enhancement have been noted (1, 14, 15), moderate to strong enhancement has frequently been reported (1, 7), as seen in 4 of 5 solid lesions in this study. Compact cellularity with a prominent capillary network may be responsible for the enhancement on CT and MR imaging (4). In this study, 5 lesions were solid and 2 lesions were partly or completely cystic. Both cystic lesions showed peripheral, nodular or rimlike enhancement. The cystic area within the lesion represents fluid-filled mucoid space (1, 7).

Various signal intensities have been shown on MR imaging of nodular fasciitis and may be a reflection of the combination of variability in cellularity, amount of collagen, amount of cytoplasm and water content of the extracellular space, and vascularity contained in the individual lesion (4). The relationship between the signal intensities on T2-weighted MR images and histologic subtypes has been advocated (1, 3–5, 7). In general, the signal intensity of the lesions with myxoid or cellular histology is higher than that of muscle on T2-weighted images, whereas lesions with fibrous histology present as markedly hypointense to the surrounding muscles on all pulse sequences. The coexistence of abundant collagen and acellularity leads to a reduction in signal intensity on T2-weighted images in fibrous type (4). In this study, of 4 lesions studied with MR imaging, the signal intensity of 2 solid lesions was isointense and hyperintense to that of muscle on T1-weighted and T2-weighted images, respectively, favoring the predominant myxoid or cellular nature of the lesions. In contrast, the signal intensity of the solid portion of the partly cystic lesion was isointense on both T1-weighted and T2-weighted images, which suggests the predominant fibrous nature of the lesion. Various signal intensities observed from the cystic portion of the lesions are probably attributed to the differences in free water content and protein concentration as well as the presence or absence of hemorrhage.

Because the imaging features of nodular fasciitis are rather nonspecific, there is a long list of radiologic differential diagnoses, which include neurogenic tumor, minor salivary gland tumor, dermoid or epidermoid, hemangioma, sarcoidosis, aggressive fibromatosis, dermatofibroma, fibrosarcoma, and malignant fibrous histiocytoma (1, 3). Once the diagnosis of nodular fasciitis has been made histologically, local excision is usually the appropriate treatment and recurrence is reported to be exceedingly rare (2, 4, 12).

Conclusions

Although rare, nodular fasciitis occurs as a discrete solid or cystic mass in the head and neck, depending on the predominant stromal components. It is most commonly found in the subcutaneous tissues, but it may be deep seated and show an aggressive behavior. Moderate to marked enhancement on CT and MR imaging is common. Although there are no pathognomonic imaging findings, nodular fasciitis should be included in the differential diagnosis of soft tissue masses in the head and neck, especially in patients with a recently developed, rapidly growing mass and a history of recent trauma.

References

1. Shin JH, Lee HK, Cho KJ, et al. **Nodular fasciitis of the head and neck: radiographic findings.** *Clin Imaging* 2003;27:31–37
2. Harrison HC, Motbey J, Kan AE, de Silva M. **Nodular fasciitis of the nose in a child.** *Int J Pediatr Otorhinolaryngol* 1995;33:257–264
3. Leung LYJ, Shu SJ, Chan ACL, et al. **Nodular fasciitis: MRI appearance and literature review.** *Skelet Radiol* 2002;31:9–13
4. Wang XL, De Schepper AMA, Vanhoenacker F, et al. **Nodular fasciitis: correlation of MRI findings and histopathology.** *Skelet Radiol* 2002;31:155–161
5. Meyer CA, Kransdorf MJ, Jelinek JS, Moser RP. **MR and CT appearance of nodular fasciitis.** *J Comput Assist Tomogr* 1991; 15:276–279
6. Hwang K, Lee DK, Lee SI. **Nodular fasciitis as a parotid tumour after face lifting.** *Br J Plast Surg* 2000;53:345–347
7. Koenigsberg RA, Faro S, Chen Xi, Marlowe F. **Nodular fasciitis as a vascular neck mass.** *AJNR Am J Neuroradiol* 1996;17:567–569
8. Oshiro Y, Fukuda T, Tsuneyoshi M. **Fibrosarcoma versus fibromatoses and cellular nodular fasciitis: a comparative study of their proliferative activity using proliferating cell nuclear antigen, DNA flow cytometry, and p53.** *Am J Surg Pathol* 1994;18:712–719
9. Montgomery EA, Meis JM. **Nodular fasciitis: its morphologic spectrum and immunohistochemical profile.** *Am J Surg Pathol* 1991;15:942–948
10. Dahl I, Jarlstedt J. **Nodular fasciitis in the head and neck: a clinicopathological study of 18 cases.** *Acta Otolaryngol* 1980;90: 152–159
11. Shimizu S, Hashimoto H, Enjoji M. **Nodular fasciitis: an analysis of 250 patients.** *Pathology* 1984;16:161–166
12. Bernstein KE, Lattes R. **Nodular (pseudosarcomatous) fasciitis, a nonrecurrent lesion: clinicopathologic study of 134 cases.** *Cancer* 1982;49:1668–1678
13. Recchia FM, Buckley EG, Townshend LM. **Nodular fasciitis of orbital rim in a pediatric patient.** *J Pediatr Ophalomol Strabismus* 1997;34:316–318
14. Barohn RJ, Kasdon DL. **Cranial fasciitis: nodular fasciitis of the head.** *Surg Neurol* 1980;13:283–285
15. Toledo AS, Rodriguez J, Cuasay NS, et al. **Nodular fasciitis of the facial region: CT characteristics.** *J Comput Assist Tomogr* 1988;12: 898–899

changed the level of BOLD signal intensity expected to 1%, the required minimum SNR decreases by a factor of 2, to 82. In a separate publication, we also showed how the BOLD sensitivity maps could be used to determine if the actual measured BOLD signal intensity change was detectable in the amygdala.[3]

What is the practical implication for real fMRI data? In Fig 1, 2 different anatomic levels of a postsurgical fMRI patient study are shown. In the first row, the mask was generated by the SIM method[1] by setting the threshold so that the tissue surrounding the brain in the raw BOLD EPI data was suppressed; signal intensity was 240. In the second row, the mask was generated by the SNR-based method,[2] with the parameters described above and an expected BOLD signal intensity change of 1% (SNR $>$ 82). Note the large differences in the mask in the region where the sinus susceptibility artifact exists, as well as near the surgical site. The third row demonstrates a very different mask based on a 0.5% BOLD signal intensity change (SNR $>$ 164). The lower level of BOLD change may be expected in patients with disease. The lower 2 rows are based on SNR, statistical confidence, and BOLD signal intensity changes, whereas the first row is based on the SIM, a number that has very little meaning.[1]

I am encouraged that the authors are concerned about the impact of image quality, artifacts, and signal intensity voids on the interpretation of clinical fMRI and have done some excellent work to illuminate this problem. We should, however, proceed carefully when developing a method to demonstrate confidence in the activation maps. Using an arbitrary method may "mask" the clinical utility of BOLD imaging.

Todd Parrish
Department of Radiology
Northwestern University Medical School
Chicago, Ill

References

1. Strigel RM, Moritz CH, Haughton VM, et al. **Evaluation of a signal intensity mask in the interpretation of functional MR imaging activation maps.** *AJNR Am J Neuroradiol* 2005;26:578–84
2. Parrish TB, Gitelman DR, LaBar KS, et al. **Impact of signal-to-noise on functional MRI.** *Magn Res Med* 2000;44:925–32
3. LaBar KS, Gitelman DR, Mesulam MM, et al. **Impact of signal to noise on functional MRI of the human amygdala.** *Neuroreport* 2001;12:3461–64

Reply:

We thank Dr. Parrish for his comments on the relationship of susceptibility and signal intensity–to-noise ratio (SNR) for confidence levels in clinical functional MR imaging (fMRI). We welcome the discussion of these issues and laud him for his comprehensive investigation of the effects of temporal SNR on blood oxygen-level dependent (BOLD) time course analyses.[1]

The statements and example of a signal intensity map (SIM) that Parrish includes in his letter, however, do not match our experience. In our study, each SIM threshold was individually matched to the patient's echo-planar imaging (EPI) data, thus eliminating the possibility for errors incurred by use of an arbitrary threshold applied across all datasets.[2] In our experience, as demonstrated by the examples for SIM formation in Figs 1–3 of our article, SIM is sensitive to regions of signal intensity loss produced by magnetic susceptibility effects when conventional echo-planar BOLD imaging is used. In all of our cases, EPI susceptibility effects in regions of frontal and basilar sinuses were delineated by the SIM. The intent of our report was to evaluate the SIM as an indication of susceptibility-induced artifact upon the interpretation of clinical fMRI mapping. These susceptibility-induced artifacts are substantially stable during the course of a fMRI time series acquisition. Therefore, within this limited assessment, the static SIM provides an adequate means for evaluation. A version of the SIM is relatively easy to produce on a clinical system and thus offers widespread utility to fMRI users.

Parrish et al[1] have applied the temporal nature of the fMRI acquisition to further evaluation of BOLD sensitivity. We appreciate the importance of their report and encourage fMRI users to become familiar with the significance of their findings. Temporal SNR measurements provide information about the BOLD signal intensity stability that is not contained within a static SIM, and indeed it is our practice to produce both types of signal intensity evaluation maps for our fMRI studies.

We regret any misunderstanding that might have led Dr. Parrish to question our report on the utility of a SIM. We are gratified by the forum for discussion of these issues, particularly when the opportunity leads toward increased awareness of limitations and capabilities for clinical fMRI.

Chad Moritz
Roberta Strigel
Howard Rowley
Victor Haughton
Department of Radiology
University of Wisconsin
Madison, Wisc

References

1. Parrish TB, Gitelman DR, LaBar KS, et al. **Impact of signal-to-noise on functional MRI.** *Magn Reson Med* 2000;44:925–32
2. Strigel RM, Moritz CH, Haughton VM, et al. **Evaluation of a signal intensity mask in the interpretation of functional MR imaging activation maps.** *AJNR Am J Neuroradiol* 2005;26:578–84

Erratum

Due to a translation error, Chung Hwan Baek's name was misspelled in the published list of authors for the article "Nodular Fasciitis in the Head and Neck: CT and MR Imaging Findings" in the November/December 2005 issue. The correct author list should be:

Sung Tae Kim, Hyung-Jin Kim, Sun-Won Park, Chung Hwan Baek, Hong Sik Byun, and Young Mo Kim. (*AJNR Am J Neuroradiol* 2005; 26:2617–23.)